C. Kennard & R.J. Leigh (Eds.)
Progress in Brain Research, Vol. 171
ISSN 0079-6123

CHAPTER 3.13

Impulsive head rotation resets oculopalatal tremor: examination of a model

Ke Liao[1], Simon Hong[2], David S. Zee[3], Lance M. Optican[2] and R.J. Leigh[1,*]

[1]*Daroff-Dell'Osso Laboratory, Veterans Affairs Medical Center and Case Western Reserve University, Department of Neurology, University Hospitals, Cleveland, OH, USA*
[2]*Laboratory of Sensorimotor Research, National Eye Institute, NIH, DHHS, Bethesda, MD, USA*
[3]*Johns Hopkins University, Baltimore, MD, USA*

Abstract: We have described a neuromimetic model of the interaction between the inferior olive (IO) and the cerebellum that accounts for symptomatic oculopalatal tremor (OPT), a disorder characterized by oscillations of the eyes (nystagmus), palate and other branchial muscles. OPT develops months after some brainstem strokes, in association with hypertrophic degeneration of the inferior olivary nucleus (IO). We hypothesized that OPT requires both (1) a pulsatile oscillator created by tighter electrotonic coupling between cells in the IO, and (2) a learned response from the cerebellar cortex that combines with the IO pulses to generate the quasi-pendular oscillations. Since the vestibular nuclei project to both IO and vestibulocerebellum, one prediction of the model is that rapid head rotations could interrupt the oscillator, effectively resetting the timing of the ocular nystagmus. The ocular oscillations in OPT vary in amplitude and phase, making it difficult to determine by Fourier analysis whether head perturbations phase-shift the nystagmus. We applied complex wavelet analysis to data from four patients with OPT and checked whether vestibular stimuli induced a change in phase of the nystagmus. First we calculated a threshold for the spontaneous rate of change of phase of OPT by comparing many segments of nystagmus waveform with their time-shifted versions, bootstrapping these arrays, and computing 95% prediction intervals for each patient. Then we compared the rate of change of phase due to each head perturbation with the threshold for that patient. To minimize the effects of the head perturbation itself on the wavelet analysis, we measured effects in a plane orthogonal to the head rotation, e.g., effects of horizontal head rotations on the torsional component of OPT. In all four patients, the rate of change of phase shift increased sharply at the time of the head perturbation, and in three the change was judged to be statistically significant. Thus, the experimental tests supported the prediction of our model for OPT.

Keywords: inferior olive; wavelets; vestibulo-ocular reflex; gap junctions; clonazepam; memantine

Introduction

The syndrome of oculopalatal tremor (OPT; previously called oculopalatal myoclonus) typically develops over weeks or months following a

*Corresponding author. Tel.: +1 216 707 6428; Fax: +1 216 231 3461; E-mail: rjl4@case.edu

DOI: 10.1016/S0079-6123(08)00632-8

brain stem or cerebellar stroke (Guillain and Mollaret, 1931; Deuschl et al., 1990). The movements of affected muscles are approximately synchronized at a rate of about 2 cycles/s (range 1.8–2.7 Hz) (Deuschl et al., 1994). The ocular oscillations (nystagmus) in OPT are smooth but irregular, usually with prominent, vertical, and torsional components, and variable disconjugacy (Kim et al., 2007). The posterior soft palate, moved by the levator veli palatini muscle, is most often affected, but eyes, facial muscles, pharynx, tongue, larynx, diaphragm, neck, trunk, and extremities may also move in synchrony. The "symptomatic" form of OPT follows a brain stem or cerebellar stroke, and is distinct from either "essential" palatal tremor, which seldom affects the eyes (Deuschl et al., 1994), or OPT arising as a feature of the syndrome of progressive ataxia (Eggenberger et al., 2001; Samuel et al., 2004).

We have developed a computational model of the interaction between the inferior olive (IO) and the cerebellum to account for symptomatic OPT (Leigh et al., 2005). The model we used had been developed to account for classic motor learning of the blink reflex (Hong and Optican, 2005; Hong et al., 2008). Based on experimental studies of inferior olivary hypertrophy (de Zeeuw et al., 1998), we first modified the model so that adjacent IO units progressively developed high-conductance soma-somatic gap junctions; this led to synchronized discharge of the population of IO neurons at $\sim$2 Hz. The model then predicted eye oscillations at 2 Hz, but they were smaller, jerkier, and more regular than those observed in patients. In the next stage in model development (Fig. 1A), pulses from the IO (black spiky curves) are transmitted to the cerebellar cortex via climbing fibres (CFs) and parallel fibres (PFs). The Purkinje cells (PC) react to the incoming signals by discharging the same temporal pattern of spikes as that of the inputs. In the third stage (Fig. 1B) coincidental arrival of PF and CF signals train the cortical PC-IN modules to learn the periodicity of the pulses. After learning, each mossy fibre (MF) pulse prompts the PC population to pause (the red wavy curve) at the expected time of the next CF signal. This periodic pause of the PC population thereby disinhibits the target vestibular neurons. Vestibular neurons now are driven from both the IO (the black spiky curve) and the PC population (the red wavy curve), and generates a signal (the red curve above the eyeball) that is a mixture of the IO pulse and PC modulation. A more complete circuit of the model is illustrated in Fig. 1C, representing a pair of oculomotor circuits; one vestibular axis is shown for simplicity.

This model successfully simulated characteristic features of the ocular oscillations of OPT: their smooth but variable waveform at 1–3 Hz, with vertical, torsional, and horizontal components, and the slow development of oscillations over the course of weeks after the stroke. However, an independent test of the model is necessary to support its validity. As inputs from the labyrinthine semicircular canals project via vestibular nuclei to both IO and the vestibulocerebellum, one prediction of the model is that a high-acceleration (impulse) head rotation would cause a major new input to the system that would shift ("reset") the phase of the ocular oscillations. Figure 2 shows the result of the model's simulation where the relatively periodic torsional component of the OPT shifts its phase after the head rotation. For a better illustration, the five cycles of periodic torsion prior to the head perturbation (in the box) have been displaced (up and to the right) to show what the phase would be if the oscillations were unaffected by the head perturbation. The post-head rotation peaks of the wavelets now do not align with the displaced peaks. We tested this model prediction in OPT.

Because the ocular oscillations of OPT have inherent randomness and non-stationary properties, we could not use classical Fourier analysis to determine phase before and after a head impulse. Accordingly, we used an alternative analysis based on the wavelet transform (WT). Being localized in both time and frequency domains, WT provides detailed information about frequency components at different times, without sacrificing resolution for either frequency or time (Torrence and Compo, 1998).

Subjects and methods

We studied four patients with OPT; their clinical features are summarized in Table 1. We used the

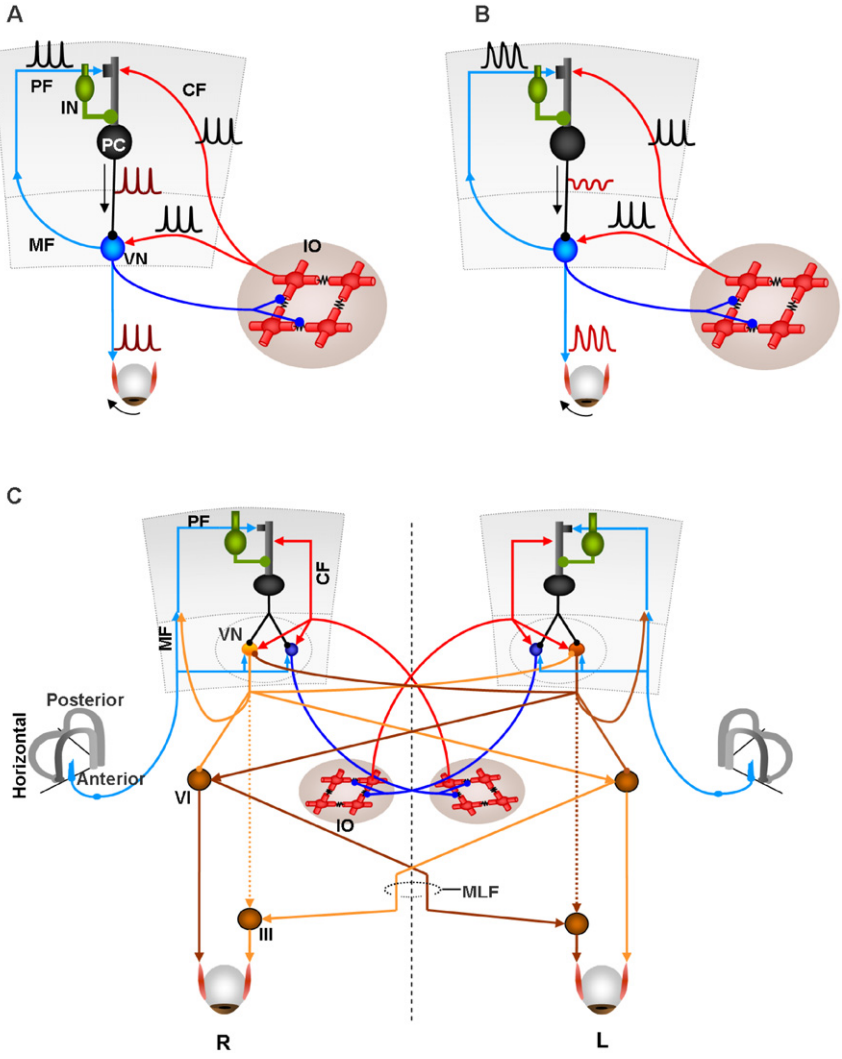

Fig. 1. Summary of the cerebellar circuit that learns the sequences of pulses from the hypertrophied inferior olive. (A) Initial stage of learning. At the beginning of learning, the pulses from the IO (black spiky curves) are simply transmitted to the cerebellar cortex via CFs and PFs. The PC simply reacts to the incoming signals by discharging the same form of spikes as that of the inputs. Note that just one projection from the IO is represented for simplicity. Also for simplicity, just one of three (anterior, posterior, and horizontal) channels is shown. Excitatory and inhibitory projections are indicated by arrow heads and spot heads, respectively. (B) Learned state of the model. The coincidental arrival of PF and CF signals train the cortical PC-IN modules to learn the periodicity of the pulses. After learning, each MF pulse prompts the PC population to pause (the red wavy curve) at the expected time of the next CF signal. This periodic pause of the PC population thereby disinhibits the target vestibular neurons. The vestibular neurons now are driven from both the IO (the black spiky curve) and the PC population (the red wavy curve), and generates a signal (the red curve above the eye ball) that is a mixture of the IO pulse and the PC modulation. (C) A more complete circuit diagram of the model. The diagram has a more detailed representation of the model showing left and right cerebellum and related connections to oculomotor structures. Both excitatory and inhibitory neurons are illustrated in VN. Note that while the inhibitory neuron connects only to the contralateral IO, the excitatory neuron sends its axons to oculomotor neurons and to the cerebellar cortex as a MF. The head rotation triggered phase reset pathway (ear canal→VN→IO) is also illustrated. The indirect projection from VN to the third cranial nucleus (III) via the contralateral sixth cranial nucleus (VI) is assumed to be stronger than the direct projection from the VN to III (dotted line). MLF: medial longitudinal fasciculus. (See Color Plate 3.13.1 in color plate section.)

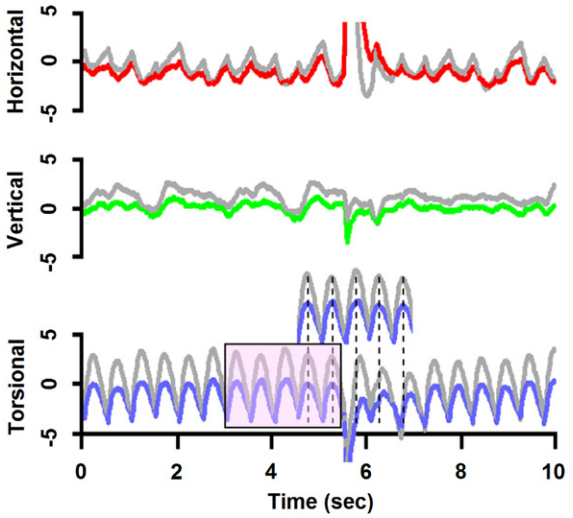

Fig. 2. Simulation of head impulse in OPT. The relatively periodic torsional component of the OPT shifts its phase after the head rotation. For comparison, the five pre-head perturbation wavelets (in box) have been displaced over around the onset of the head perturbation. The simulated head perturbation is a quick horizontal rotation. The overshooting horizontal trace marks the onset of the head rotation. Note that the post-head rotation peaks of the wavelets now do not align with the displaced ones. Grey traces represent right eye, coloured traces represent left eye. Vertical scale: deg/s. (See Color Plate 3.13.2 in color plate section.)

magnetic field/search coil technique to measure 3-D eye and head rotations, as previously described (Steffen et al., 2000). Each subject viewed a central visual target (laser spot projected onto a tangent screen at a distance of 125 cm) with each eye in turn. Coil signals were low-pass filtered (0–150 Hz) prior to digitization at 500 or 1000 Hz. During each experiment, subjects were asked to fixate the central visual target for 15–30 s. Next, the investigator manually applied impulsive head rotations to the subjects approximately every 5 s for 30 s.

We analysed the spectrum information of the signal before and after the head perturbation to evaluate the change in energy. In order to determine the characteristic spectrum of the resting nystagmus, we chose the fixation period of each trial, and picked out a series of saccade-free eye movements (using a criterion of eye velocity less than 40 deg/s). After re-sampling these movements, we obtained a total number of 100 1 s slices, which allowed us to estimate their spectrum and confidence interval. Since the number of the slices is large (1 0 0), we fitted it with a normal distribution. We then calculated the spectrum in a series of 1 s slices after each head perturbation, and compared their spectrum with that of nystagmus during fixation (head stationary).

Table 1. Summary of clinical findings and responses of nystagmus to head impulse stimuli

Age/sex/ duration	Clinical data	Medicines	Peak PSCR at head perturbation[a]	Threshold[a]
P1 50/F/4 year	4 year history of progressive ataxia and visual jumping beginning after a viral infection	Gabapentin atenolol	1032[b]	870
P2 46/M/18 months	Pontine and midbrain haemorrhage; eye symptoms began between 1 and 4 months after haemorrhage	Memantine, clonazepam	917[b]	900
P3 55/M/15 months	Pontine haemorrhage, eye symptoms began shortly after stroke	Norvasc, lopressor, carbidopa and levodopa at bedtime	955[c]	238
P4 57/M/3 year	Bilateral vertebral occlusion causing left anterior medullary and pontine infarction; eye symptoms began 1 year after stroke	Aspirin	95	797

[a]Units of rate of change of phase shift (PSCR) are degrees of phase shift per second. Threshold is 95% prediction interval of phase shift during fixation.
[b]PSCR exceeded threshold.
[c]Although PSCR exceeded threshold, frequent saccades, and blinks also did so.

The easiest way to measure the phase shift of these ocular oscillations is to compare the waveform with its own shifted version. The OPT oscillations usually cycle around a fixed frequency within an epoch of a few seconds, so by shifting the OPT waveform on the time axis by a few cycles, we can predict the phase of the waveform if it were not perturbed. (Testing during the fixation period showed that phase changes between the original and shifted waveforms were relatively small within a unit time period.) Thus, we shifted the ocular oscillation by a few cycles and compared its phase with that of its un-shifted version before and after the head perturbation.

We also calculated the rate of change of phase shift, which is the derivative of the phase difference between the shifted OPT oscillation and its un-shifted version during the head perturbation. Since wavelet coherence analysis results in 2-D data (time and frequency), and the OPT oscillations lie within a certain range of frequencies, we took a circular mean on the frequency axis to convert to 1-D data before we performed a derivative operation. As we observed, the OPT oscillations have their major frequency components at 1–4 Hz, corresponding to a period of 0.25–1.0 s. A circular mean is defined as:

$$a_m = \text{atan}(X, Y) \text{ with } X = \sum_{i=1}^{n} \cos(a_i) \text{ and}$$

$$Y = \sum_{i=1}^{n} \sin(a_i)$$

where a_m is the circular mean of a_i ($i = 1$ to n). The circular mean is used here to calculate the mean of trigonometric angles. We calculated a threshold for the spontaneous rate of change of phase of OPT by comparing many segments of OPT waveform with their time-shifted version, bootstrapping these arrays, and computing 95% predictions intervals for each patient. Then we compared the rate of change of phase (PSCR) occurring with each head perturbation with the threshold for that patient.

Results

An example of the ocular oscillations of one patient is shown in Fig. 3A. Note that in this patient the torsional component of the oscillation was the largest. We measured changes in the torsional oscillations in response to orthogonal (horizontal or vertical) head impulses; in this way, artefacts induced by the head rotation were minimized.

After analysing the eye movement with the wavelet decomposition and reconstruction package in Matlab (The Mathworks, Inc.), we found the energy of OPT oscillation only resides from level 6 to level 8 of the wavelet decomposition, corresponding to a frequency range of approximately 1–4 Hz (Liao et al., 2008). The energy that resides in levels 9–12 corresponds to the lower frequency components in the waveform, and the residual energy is of high frequency and lower amplitude, which can be ignored as the noise. Thus, our analysis will be focused on the spectrum of level 6–8 of the wavelet decomposition. A comparison of the energy of resting nystagmus versus that of OPT nystagmus after the head perturbation indicates that the energy of the OPT oscillation was not changed by the head perturbation.

As described above, the original eye movement was shifted by two or more cycles to compare the phase difference between the original and the shifted waveform. Of the four patients studied, two (P1 and P2, Table 1) showed phase difference changes that exceeded the calculated threshold at the moment of the head perturbation. Thus, in Fig. 3B, PSCR is greater than the threshold (870 deg/s) only during the head perturbation, whereas before and after the head perturbation the PSCR is small and well below the threshold. In the two other patients, spikes of PSCR were also evident with head perturbations. However, P3 also exceeded the threshold during frequent saccades and blinks. P4, alone, did not exceed threshold during head perturbations.

Discussion

We set out to test a new model for OPT (Fig. 1) by applying impulsive head rotations. The model predicted that such vestibular stimuli would induce changes in the oscillations that would be evident as phase shifts in the waveform proceeding versus following the head rotation (Fig. 2). Since

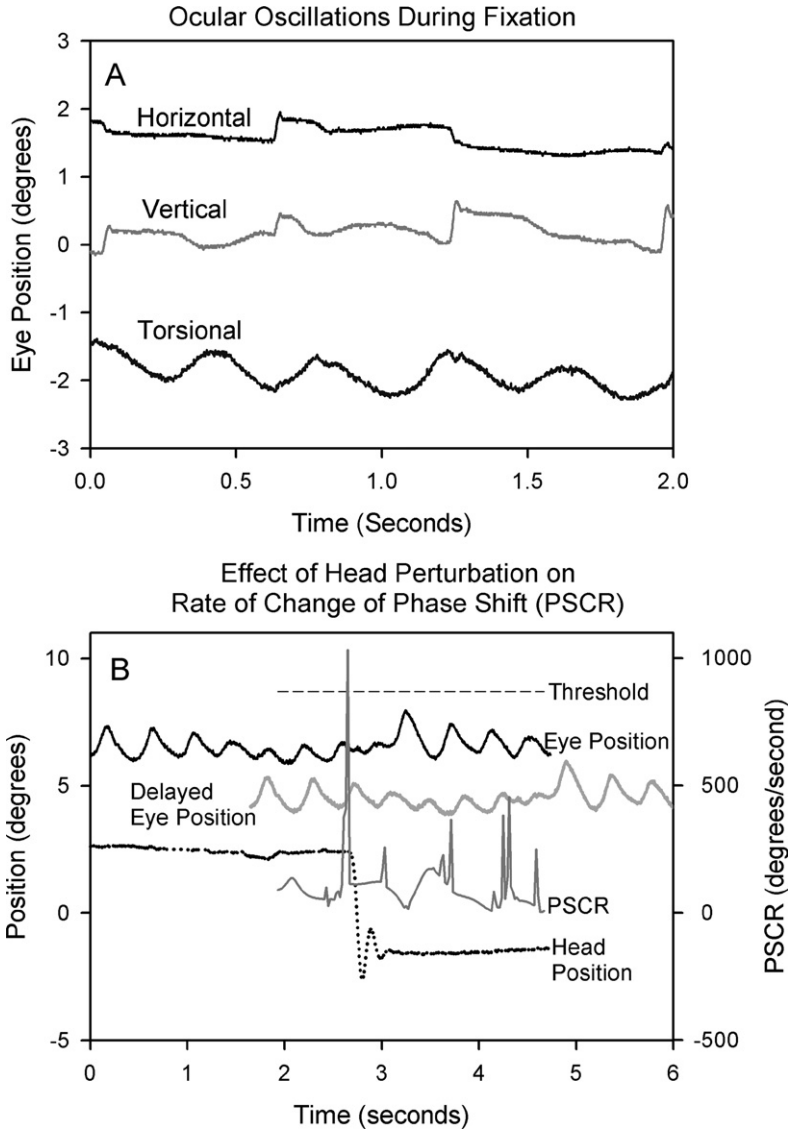

Fig. 3. OPT and impact of head rotation. (A) Example of ocular oscillations of Patient 1; note how the torsional component is the largest; each channel has been offset in position to aid clarity of display. (B) Example of effect of one head impulse on ocular oscillations of Patient 1. The upper black channel represents torsional eye position, whereas the upper gray channel is the same segment of eye position plotted with a delay of 1.65 s and offset of 2 deg in position for ease of comparison. The horizontal head perturbation is shown in the lower black channel. The rate of change of phase shift (PSCR) between the ocular oscillations and their shifted version is shown in the lower gray channel; note separate scale at right. At the time of the head impulse, PSCR exceed a threshold of 95% prediction interval for ocular oscillations during attempted fixation of a stationary target.

OPT has non-periodic and non-stationary properties, it was not possible to simply compare the ocular oscillations with a reference sine wave, as has been done in prior studies of periodic ocular oscillations (e.g., Das et al., 2000). Accordingly, we chose an approach that applied complex wavelet analysis (Torrence and Compo, 1998; Liao et al., 2008).

In all four patients, we detected a substantially greater rate of change of phase during the head impulse stimulus compared with changes of phase that occurred spontaneously during attempted fixation with the head stationary (Fig. 3). In three patients the rate of change of phase was statistically significant (Table 1). In one patient, phase shifts also exceeded threshold during frequent blinks and saccades. It seems possible that the analytic technique that we employed in this study may provide clearer results by asking patients to refrain from blinking and allowing a minimal of five OPT cycles between successive head impulses. Furthermore, this wavelet analysis approach might also be applied to determine whether other eye movements, such as saccades, cause shifts of the OPT waveform, which our results and prior studies (Kim et al., 2007) suggest.

Another way to test our model is to study the effects of drugs (Hong et al., 2008). In occasional patients, OPT is suppressed by a range of medicines, including memantine, which blocks NMDA receptors, and clonazepam, which has GABAergic properties (Leigh and Zee, 2006). In one such patient, with ocular oscillations following pontine haemorrhage, positron emission tomography (PET) demonstrated increased regional cerebral metabolic rate of glucose utilization (rCMRGlu) in the right IO (Yakushiji et al., 2006). Treatment with clonazepam reduced the amplitude of the ocular oscillations, and decreased rCMRGlu in the contralateral inferior cerebellar vermis, but not in the IO. If clonazepam blocked the cerebellar output, the nystagmus would only be driven by the IO output, and so its amplitude would be reduced. A complementary approach would be to study the effects of new drugs that act on the gap junctions of the IO. At present, antimalarial drugs are known to block gap-junctions (Cruikshank et al., 2004), and it seems likely that other agents will become available that could then be subjected to clinical trials for OPT.

To summarize, we have developed a hypothesis for the mechanism underlying the ocular oscillations of the syndrome of OPT, which is associated with inferior olivary hypertrophy. We simulated the ocular oscillations with a mathematical model of IO — cerebellar interactions based on the ideas that (1) hypertrophied olivary neurons become tightly coupled by an increase in gap junctions, leading to periodic synchronized discharge and (2) gratuitous learning of this IO signal by cerebellar cortex modulates the ocular oscillation waveform. An experiment test confirmed model predictions concerning the effects of vestibular stimuli on OPT. The model also makes predictions about potential drug treatments that could be evaluated in clinical trials.

Acknowledgement

This work is supported by NIH grant EY06717; the Office of Research and Department of Veterans Affairs; Evenor Armington Fund; Intramural Division of the National Eye Institute, NIH, DHHS.

References

Cruikshank, S.J., Hopperstad, M., Younger, M., Connors, B.W. and Spray, D.C. (2004) Potent block of Cx36 and Cx50 gap junction channels by mefloquine. Proc. Natl. Acad. Sci. U.S.A., 33: 12365–12369.

Das, V.E., Oruganti, P., Kramer, P.D. and Leigh, R.J. (2000) Experimental tests of a neural-network model for ocular oscillations caused by disease of central myelin. Exp. Brain Res., 133: 189–197.

Deuschl, G., Mischke, G., Schenck, E., Schulte-Monting, J. and Lucking, C.H. (1990) Symptomatic and essential rhythmic palatal myoclonus. Brain, 113(Pt 6): 1645–1672.

Deuschl, G., Toro, C., Valls-Solo, J., Zee, D.S. and Hallett, M. (1994) Symptomatic and essential palatal tremor. 1. Clinical, physiological and MRI analysis. Brain, 117: 775–788.

de Zeeuw, C.I., Simpson, J.I., Hoogenraad, C.C., Galjart, N., Koekkoek, S.K.E. and Ruigrok, T.J. (1998) Microcircuitry and function of the inferior olive. Trends Neurosci., 21: 391–400.

Eggenberger, E., Cornblath, W. and Stewart, D.H. (2001) Oculopalatal tremor with tardive ataxia. J. Neuroophthalmol., 21: 83–86.

Guillain, G. and Mollaret, P. (1931) Deux cas myoclonies synchrones et rhythmées vélo-pharyngo-laryngo-oculodiaphragmatiques: le problèm anatomique et physiolopathologique de ce syndrome. Rev. Neurol. (Paris), 2: 545–566.

Hong, S., Leigh, R.J., Zee, D.S. and Optican, L.M. (2008) Inferior olive hypertrophy and cerebellar learning are both needed to explain ocular oscillations in oculopalatal tremor. Prog. Brain Res. (this volume): 219–226.

Hong, S.Y. and Optican, L.M. (2005) New cellular mechanisms for multiple time-scale adaptation in cerebellum. Soc. Neurosci. Abstr., 933.7.

Kim, J.S., Moon, S.Y., Choi, K.D., Kim, J.H. and Sharpe, J.A. (2007) Patterns of ocular oscillation in oculopalatal tremor imaging correlations. Neurology, 68: 1128–1135.

Leigh, R.J., Hong, S., Zee, D.S. and Optican, L.M. (2005). Oculopalatal tremor: clinical and computational study of a disorder of the inferior olive. Soc. Neurosci. Abstr., 933.8.

Leigh, R.J. and Zee, D.S. (2006) The Neurology of Eye Movements (Book/DVD) (4th edn.). Oxford University Press, New York.

Liao, K., Hong, S., Zee, D.S., Optican, L.M. and Leigh, R.J. (2008). Using wavelet analysis to evaluate effects of eye and head movements on ocular oscillations. In: Leigh, R.J. and Devereaux, M.W. (Eds.), Advances in Understanding Mechanisms and Treatment of Infantile Forms of Nystagmus. Oxford University Press, New York (in press).

Samuel, M., Torun, N., Tuite, P.J., Sharpe, J.A. and Lang, A.E. (2004) Progressive ataxia and palatal tremor (PAPT): clinical and MRI assessment with review of palatal tremors. Brain, 127: 1252–1268.

Steffen, H., Walker, M.F. and Zee, D.S. (2000) Rotation of Listing's plane with convergence: independence from eye position. Invest. Ophthalmol. Vis. Sci., 41: 715–721.

Torrence, C. and Compo, G.P. (1998) A practical guide to wavelet analysis. Bull. Am. Meteorol. Soc., 79: 61–78.

Yakushiji, Y., Otsubo, R., Hayashi, T., Fukuchi, K., Yamanda, N., Hasegawa, Y. and Minematsu, K. (2006) Glucose utilization in the inferior cerebellar vermis and ocular myoclonus. Neurology, 67: 131–133.